Int. J. Electrochem. Sci., 13 **(2018)** 5151 – 5163, doi: 10.20964/2018.06.29

International Journal of
ELECTROCHEMICAL
SCIENCE
www.electrochemsci.org

Electrochemical Behaviour of Iron in Simulated Acid Rain in Presence of *Achillea Millefolium* L.

Zora Pilić[*], *Ivana Martinović and Gloria Zlatić*

Department of Chemistry, Faculty of Science and Education, University of Mostar, Mostar, Bosnia and Herzegovina
[*]E-mail: zora.pilic1@gmail.com

Received: 10 February 2017 / *Accepted:* 24 March 2018 / *Published:* 10 May 2018

The effect of the aqueous extract of *Achillea millefolium* L. (AM) on the electrochemical behaviour of iron in a simulated acid rain solution (pH 4.5) was studied by electrochemical techniques cyclic voltammetry, potentiodynamic polarization and electrochemical impedance spectroscopy. Experiments were carried out over a wide range of AM concentrations. The results of all techniques showed that AM extract contributes to iron passivation. The films formed in the presence of AM extract were thinner and more resistive then the films formed in pure simulated acid rain solution. The AM extract adsorbed on the iron according to the Freundlich isotherm. The thermodynamic data indicated physical adsorption of the AM extracts on the iron surface. The concentration of the metallic ions released into solution, measured by atomic absorption spectroscopy, was in accordance with the results obtained from the electrochemical techniques.

Keywords: Iron; *Achillea millefolium* L. extract; Simulated acid rain; Electrochemical methods; *Atomic absorption spectrometry*

1. INTRODUCTION

Iron and its alloys represent an important category of materials due to their high technological value and wide range of industrial applications. The problem of corrosion of these materials is a significant research topic, its protection against corrosion has attracted much attention [1-9]. The corrosion behaviour of metals and alloys depends on the properties and stability of the surface oxide layer. So, properties of surface layer have sparked the researchers' interest for the phenomenon of its formation and growth.

It is generally accepted that the passive film on iron consists basically of two layers, Fe_3O_4 inner layer and γ-Fe_2O_3 outer layer [10, 11]. The good corrosion resistance of stainless steel in various

solutions is due to the highly protective passive (oxide) film that is the key factor for its corrosion stability. Several authors [12-16] have shown that the passive film on stainless steel is composed of a chromium oxide enriched inner layer and an iron oxide enriched outer layer. The formation of oxide film is complex electrooxidation process, which depends on a large number of variables, such as: the pretreatment of the metal surface, the electrode potential, the polarization time, the temperature, chemical composition and the pH of the electrolyte. However, in the presence of aggressive ions [1, 3, 17, 18] or other environments like acid rain [18-20] the protective layer can be destroyed and corrosive attack takes place.

One of the methods of corrosion protection is the application of corrosion inhibitors. The protection of iron and its alloys against the corrosion with different kind of inhibitors has been widely studied [21-26], but many commercial inhibitors have toxic properties and have adverse effects on the environment. New nontoxic and environment friendly inhibitors are in the focus of intensive researches in the last time [25, 26]. Naturally occurring antioxidants like phenolic compounds are non toxic, easily biodegradable and renewable and hence can be potentially used as effective corrosive inhibitors. Numerous studies reported that natural corrosion inhibitors are mostly obtained from medicinal plants, aromatic spices, and herbs [27, 28]. In corrosion systems metal/aqueous media, phenolic compounds exhibit a dual character. They act as corrosion inhibitors in acidic solutions and on rust covered steel in neutral solutions. On the other hand on bare steel in neutral solutions they act as corrosion activators [22]. The importance and wide application of iron and its alloys have provided an incentive for research into the possibility of inhibition of corrosion by means of natural antioxidant from *Achillea millefolium* L. leaves. This plant is a medicinal plant of Mediterranean origin with outstanding antioxidant and antiplasmodial properties [27].

In our earlier paper [20] we studied electrochemical behaviour of iron and AISI 304 stainless steel in acid rain (pH 4.5) solution. This study is a continuation of electrochemical research of iron in acid rain in the presence of a Mediterranean plant *Achillea millefolium* L. as a potential corrosion inhibitor. The *Achillea millefolium* L. is a medicinal plant of Mediterranean origin with outstanding antioxidant and antiplasmodial properties [27] because it contains different phenolic compounds [27].

2. EXPERIMENTAL PROCEDURE

Spectroscopically pure iron was used as a working electrode. The surface area of the Fe sample, exposed to the electrolyte, was 0.636 cm^2. The electrode was mechanically abraded by 1200 grade emery paper, degreased with ethanol in an ultrasonic bath and rinsed with ultra pure water (18.2 MΩ cm, produced by Millipore Simplicity UV Water Purification System). Prior to each measurement Fe electrode was polarized at –1.20 V vs. Ag | AgCl | 3 M KCl electrode for 15 seconds to remove an air-formed oxide from the surface.

The basic electrolyte was a simulated acid rain solution. Chemical composition of the simulated acid rain [29] is given in Table 1. The pH value of solution was 4.5 and electrical conductivity 1.306 mS cm^{-1}. pH value was adjusted by the addition of the appropriate amount of 0.5 mol L^{-1} H_2SO_4. All chemicals were of p.a. purity and obtained from Sigma Aldrich.

Table 1. Chemical composition of the simulated acid rain solution (g L^{-1}).

NH_4NO_3	$MgSO_4 \cdot 7H_2O$	Na_2SO_4	$KHCO_3$	$CaCl_2 \cdot 2H_2O$
0.13	**0.31**	**0.25**	**0.13**	**0.31**

Experiments were performed in simulated acid rain solution, pH 4.5, without and with the addition of *Achillea millefolium* L. *(Asteraceae)*. The aerial parts of *A. millefolium* L. were collected during summer 2014, in Goranci (Mostar, BiH). A AM specimen was dried in air for two weeks. Extract of plant material was prepared after 3 h maceration at room temperature. The concentrations of the *Achillea millefolium* L. extract were 0.01, 0.10, 0.50 and 1.00 g L^{-1}.

The electrochemical measurements were performed at room temperature in a standard three electrode cell. The counter electrode was a platinum electrode and the reference electrode, to which all potentials in the paper are referred, was an Ag | AgCl | 3 M KCl.

The electrochemical behaviour of iron electrode in simulated acid rain solution, without and with different concentrations of *Achillea millefolium* L. (AM extract) was studied by the combination of electrochemical techniques, cyclic voltammetry (CV), potentiodynamic polarization (PP) and electrochemical impedance spectroscopy (EIS). All measurements were performed with an Autolab PGSTAT320N controlled by a personal computer using Nova 1.5 software. For Fe electrode CV measurements were carried out in the potential range between –1.20 V and –0.10 V. The potentiodynamic polarization measurements were performed in the potential range from -250 mV to 250 mV near corrosion potential with the scanning rate of 0.5 mV s^{-1}.

EIS measurements were carried out at the open circuit potential using 10 mV AC perturbation (rms) in the frequency range of 10 kHz to 5 mHz. Prior to each measurement the electrodes were stabilized for 30 min at the selected potentials. This procedure gave good reproducibility of results.

The concentrations of the iron ions released into simulated acid rain solution after 60 minutes of specimens' immersion at open circuit potentials were obtained by atomic absorption spectrometry (AAS). Since the EIS measurements lasted approx. 60 minutes, the concentration of released ions was determined after this period of time.

3. RESULTS AND DISCUSSION

3.1. Cyclic Voltammetry

Cyclic voltammograms for the Fe electrode in simulated acid rain solution, pH 4.5, in the absence and presence of *Achilea millefolium* L. (AM) extract are shown in Figure 1.

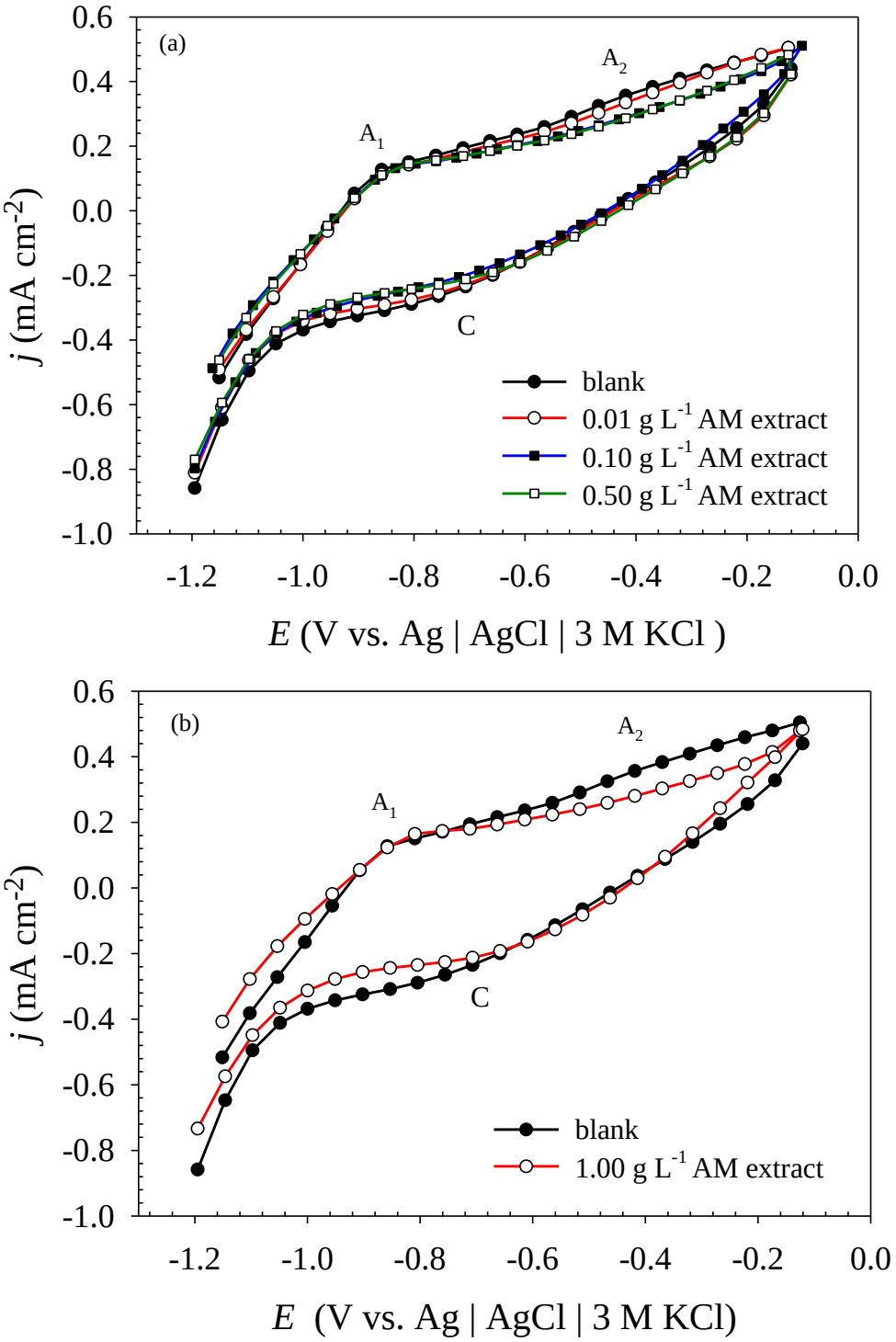

Figure 1. Cyclic voltammograms of Fe electrode in a simulated acid rain solution, pH 4.5, containing different concentrations of AM extract (shown in figure); ν = 40 mV s^{-1}.

As can be seen from Figure 1, two oxidation peaks of Fe electrode in a simulated acid rain solution are observed without AM extract. The first oxidation peak, A_1, at around –0.90 V, is related to the formation of a non-protective $Fe(OH)_2$ layer [5, 30]. The second anodic peak A_2, at around –0.45 V, is related to the formation of a Fe(III) oxide. In the reduction scan a broad cathodic peak, C, can be observed. The current peak C represents two overlapping current peaks [26]. The first one may be

attributed to the reduction of Fe(III) species to Fe(II), while the second current peak may be attributed to the reduction of Fe(II) to Fe(0). Our previous research [20] showed that the reduction of anodically formed oxide layer is not complete.

It can be seen from the Fig. 1 that the addition of AM extract (0.01, 0.10, 0.50 and 1.00 g L^{-1}) causes a decrease in the current density, i.e. shifts both the anodic and cathodic current densities. This may be ascribed to adsorption of inhibitor on metal surface. The literature indicates that natural polyphenolic compounds readily form complexes with di- and trivalent metal ions [26, 31]. The analysis of composition of the *Achilea millefolium* L. by means of high-performance liquid chromatography (HPLC) [27, 32, 33] has confirmed the presence of the natural polyphenolic compounds. The inhibitory action of the AM extract considered could therefore be explained by the formation of complexes in the form of chelates with Fe^{3+} ions and subsequent precipitation of the complex formed at the surface of the metal. The adsorption of phenols on metal surface was also confirmed by Raman Spectroscopy [34]. The thin layer formed presents a physical barrier preventing electrolyte action on the metal surface [26].

From the CV experiments, it is possible to estimate the thickness of the anodic film formed on Fe in acid rain solution with and without AM extract. Integration of anodic area of cyclic voltammograms (Fig 1.) gives the total charge of the oxidation process. From this charge the thickness of the surface film can be calculated according to Faraday's law. Under assumption that the surface layer on iron is mostly composed of Fe_2O_3 oxide [1, 26] and using literature data for the density (ρ = 5.24 g cm^{-3} [35]) and molar mass of Fe_2O_3 (M = 159.68 g mol^{-1}) the film thickness, d was calculated according to the equation:

$$d = \left(\frac{M}{\rho \, z \, F} \right) \frac{Q_A}{\sigma} \tag{1}$$

where z is the number of electrons, F is the Faraday constant and σ is the roughness factor of the surface (σ = 2). The obtained values are shown in Table 2 and are in a good agreement with the literature [5, 20, 26].

The surface coverage, θ and inhibition efficiency, η of AM extract were calculated from determined anodic charges (Fig. 1) according to relations:

$$\theta = \frac{Q_A - Q_A(\mathrm{AM})}{Q_A} \tag{2}$$

$$\eta = \theta \cdot 100 \tag{3}$$

where Q_A and Q_A(AM) represent anodic charges in the absence and presence of AM extract, respectively. Table 2 shows the values of surface coverage, θ and inhibition efficiency, η. Increase in concentration of AM extract leads to decrease in anodic charges and film thickness, which indicate that the inhibition efficiency of AM extract increases with the increase in its concentration. Table 2 also reveals that inhibition efficiency of AM extract in simulated acid rain is very low with its maximum of 26 % at concentration of 1.00 g L^{-1} AM extract.

Table 2. Charge of the anodic processes, thickness of the oxide film, surface coverage and inhibition efficiency calculated from the data shown in Figure 1.

γ (AM extract) / g L^{-1}	Q_A / mC cm^{-2}	d / nm	θ	η /%
0	**23.468**	**6.176**	**-**	**-**
0.01	**21.034**	**5.535**	**0.1037**	**10.37**
0.10	**19.069**	**5.018**	**0.1875**	**18.75**
0.50	**18.163**	**4.780**	**0.2260**	**22.60**
1.00	**17.366**	**4.570**	**0.2600**	**26.00**

3.2. Potentiodynamic polarization

Figure 2 shows the potentiodynamic polarization curves for the Fe electrode in simulated acid rain solution, pH 4.5, in the absence and presence of *Achilea millefolium* L. (AM extract) in different concentrations. These results indicate that the increase in AM extract concentration leads to decrease in corrosion current density (Table 3).

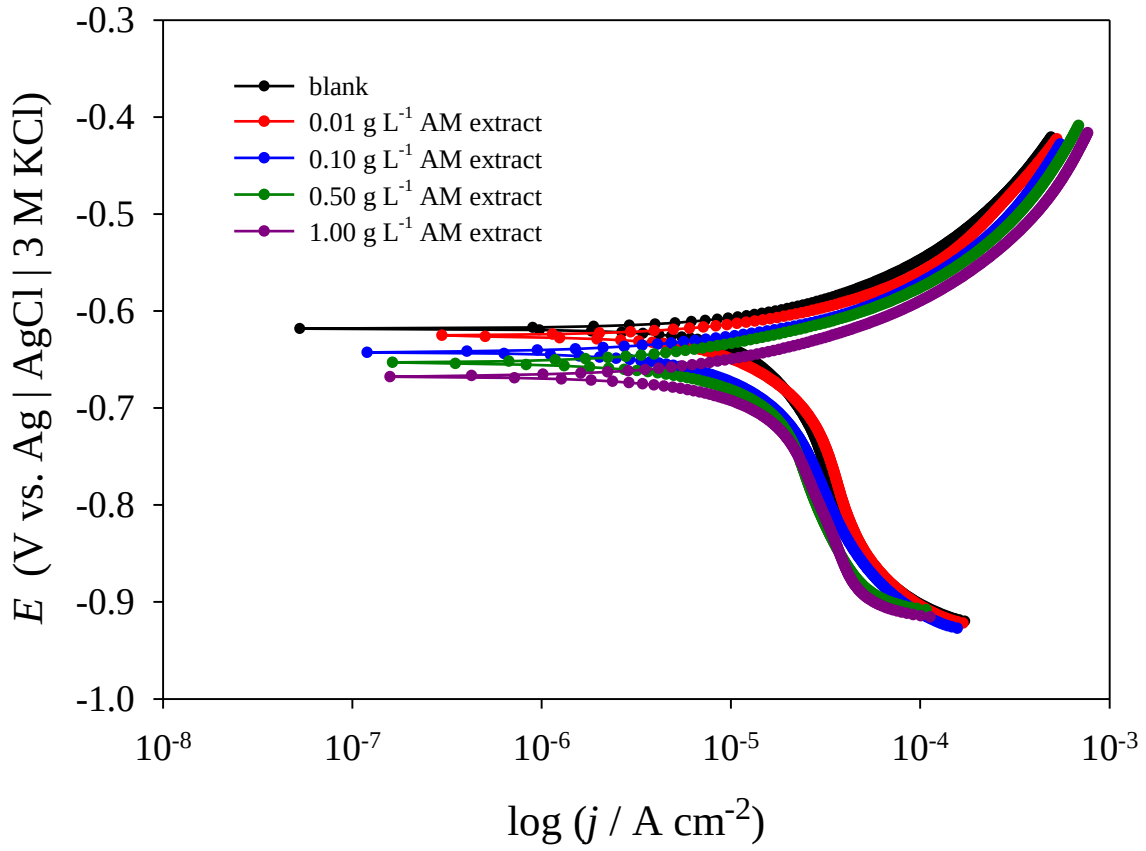

Figure 2. Potentiodynamic polarisation curves of Fe electrode in a simulated acid rain solution, pH 4.5, containing different concentrations of AM extract (shown in figure).

Corrosion parameters values were obtained by Tafel extrapolation method. The surface coverage and inhibition efficiency of AM extract were calculated using following equations:

$$\theta = \frac{j_{corr} - j_{corr}(AM)}{j_{corr}} \quad (4)$$

$$\eta = \theta \cdot 100 \quad (5)$$

where j_{corr} and j_{corr}(AM) represent corrosion current density in the absence and presence of AM extract, respectively. Calculated values are presented in Table 3.

Table 3. Corrosion potential, corrosion density, surface coverage and inhibition efficiency obtained from the data shown in Figure 2.

γ (AM extract)/ g L^{-1}	E_{corr} (V)	j_{corr} (A cm^{-2})	θ	η (%)
-	-0.643	$6.33 \cdot 10^{-6}$	-	-
0.01	-0.644	$5.61 \cdot 10^{-6}$	0.114	11.4
0.10	-0.637	$5.14 \cdot 10^{-6}$	0.188	18.8
0.50	-0.648	$5.00 \cdot 10^{-6}$	0.210	21.0
1.00	-0.667	$4.85 \cdot 10^{-6}$	0.234	23.4

3.3. Adsorption isotherm and free energy of adsorption

It is widely acknowledged that adsorption isotherms provide insight into the mechanism of corrosion inhibition. Assuming a direct relationship between inhibition efficiency and surface coverage for different inhibitor concentrations, data obtained from CV measurements were adapted to determine the adsorption characteristics of AM extract on Fe in a simulated acid rain solution.

To clarify the nature of adsorption, theoretical fitting to different isotherms was undertaken. It is found that the results follow the Freundlich isotherm (Fig. 3). The relationship between the surface coverage, θ, the equilibrium adsorption constant, K and the inhibitor concentration, γ is given by the following equations:

$$\theta = K\gamma^n \quad (6)$$

where $0 < n < 1$, or

$$\log\theta = \log K + n\log\gamma \quad (7)$$

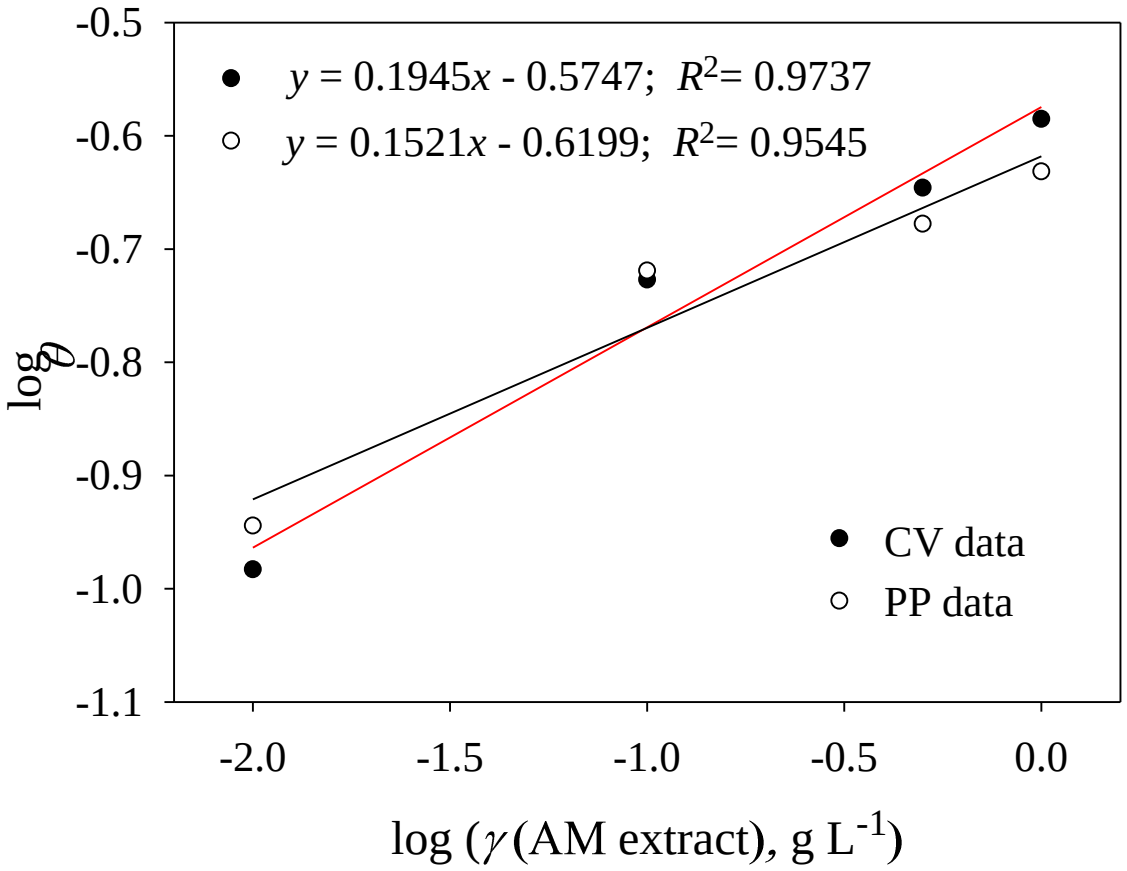

Figure 3. Freundlich adsorption isotherm for AM extract.

The equilibrium adsorption constant is related to the free energy of adsorption $\Delta G°$ [36, 37] by:

$$\Delta G^{\circ} = -RT \ln[(1000(\text{g/L}) \cdot K(\text{L/g})] \quad (8)$$

where the value of 1000 is the mass concentration of water in the solution in g L, R is the universal gas constant and T is the absolute temperature. The calculated values free energy of adsorption from CV data ($\Delta G°$ = –13.835 kJ mol^{-1}) and from PP data ($\Delta G°$ = –13.587 kJ mol^{-1}) indicates physical adsorption of the organic compounds from AM extract on the iron surface.

This multiplication was used to nullify the unit of K (L/g) with 1000 g of water per L of aqueous solution. Some researchers [36, 37] had multiplied K (L/mol) by 55.5 (number of moles of water per liter, 1L = dm^3), for the same reason ($\Delta G^{\circ} = -RT \ln(55.5 \cdot K)$).

3.4. Electrochemical impedance spectroscopy

Impedance measurements on Fe in a simulated acid rain, pH 4.5, in the absence and presence of AM extracts were performed at the open circuit potential, E_{OCP} (Fig. 4).

In the high-frequency region the, log |Z| against log f relationship approaches zero, and the phase angle values falling rapidly toward 0° with increasing frequency. The high frequency limit (f > 10^3 Hz) corresponds to the electrolyte resistance (R_Ω) which was 50 Ω cm^2 in all cases. In the medium

frequency region, a linear relationship between log |*Z*| against log *f* is observed. The phase angle maxima (less than 60°), indicates poor capacitive properties of the surface films. In the low-frequency range, the region where log |Z| does not depend on log *f* is not reached up to 10^{-1} Hz, for pure acid rain solution and for 0.01 and 0.10 g L^{-1} AM extracts solution. For solution of 0.50 and 1.00 g L^{-1} AM extracts, inside the low frequency range, the slope of the log |*Z*| vs. log *f* and the phase angle maximum close to –45° indicate Warburg-like behaviour. Warburg impedance can be explained by the diffusion process through the surface film.

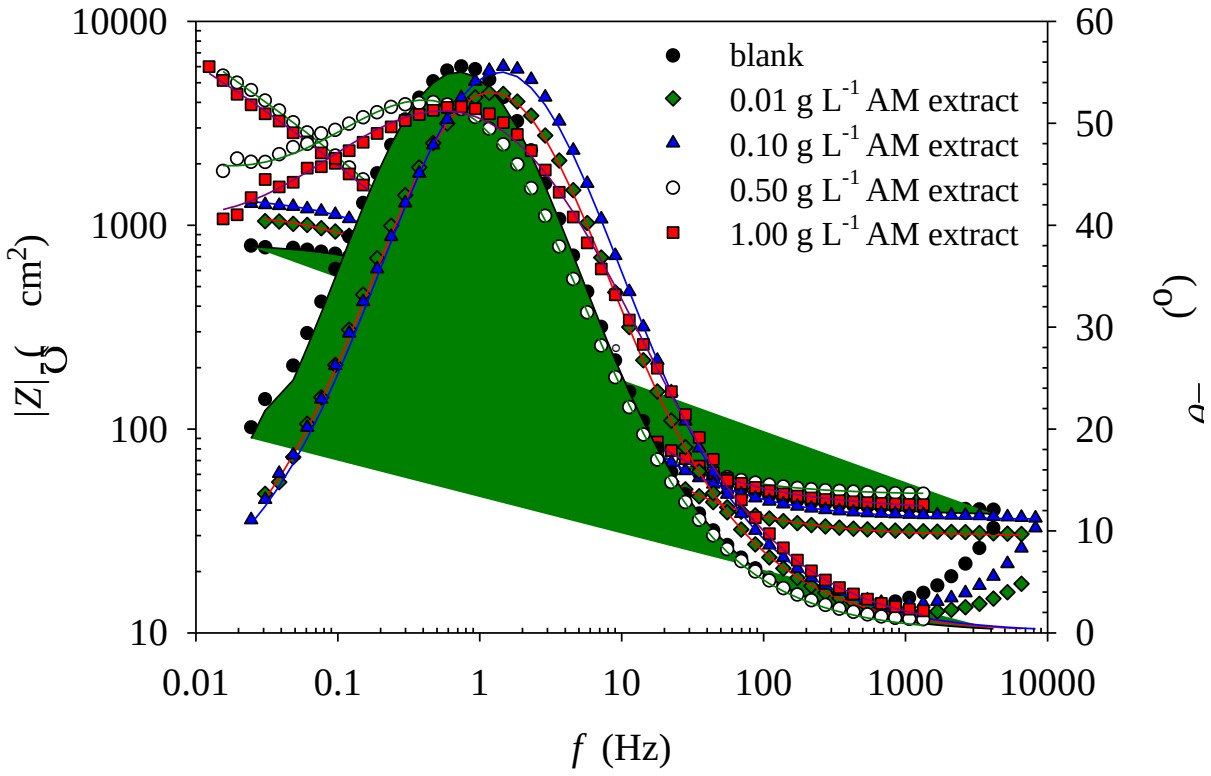

Figure 4. Impedance spectra of Fe electrode recorded at the E_{OCP} in a simulated acid rain solution, containing different concentrations of AM extract (shown in figure).

The impedance spectra of Fe in pure acid rain solution and in the presence 0.01 and 0.10 g L^{-1} AM extracts, may be described by a simple electric equivalent circuit (EEC) shown in Fig. 5a and the resultant EIS parameters are given in Table 4. EEC consists of ohmic resistance, R_Ω in a serial connection with a CPE/R_1 parallel combination representing the capacity and the charge-transfer resistance of the surface layer. For fitting, constant phase element (*CPE*) was used instead of an ideal capacitance element to compensate surface heterogeneities [38, 39]. Its impedance may be defined: $Z_{CPE}(\omega) = \left[Q(j\omega)^n\right]^{-1}$, where *Q* is a constant, ω is the angular frequency and *n* is the *CPE* power with values between 0.5 and 1 [40]. When $n = 1$, the *CPE* describes an ideal capacitor with *Q* equal to the capacitance (*C*). For $0.5 < n < 1$, the *CPE* describes a distribution of dielectric relaxation times in frequency space, and when $n = 0.5$ the *CPE* represents a Warburg impedance [41]. The total

impedance of Fe in pure acid rain solution and in the presence of 0.01 and 0.10 g L^{-1} AM extracts, recorded at the open circuit potential is given by:

$$Z_{\text{tot}} = R_{\Omega} + \frac{R_1}{R_1 Q(j\omega)^n + 1} \tag{9}$$

The impedance spectra of Fe in 0.50 and 1.00 g L^{-1} AM extracts solution, may be described by EEC shown in Fig. 5b and the resultant EIS parameters are given in Table 4.

In this case, EEC consists of ohmic resistance, R_{Ω} in a serial connection with two-time constants. The first-time constant is the result of a charge transfer process at the surface layer/acid rain interface. The second-time constant, in the low frequency region, results from ion transport through the surface layer and it is represented by constant phase element (CPE_2). For the exponent $n_2 \approx 0.5$ the constant phase element CPE_2 represents Warburg impedance. The total impedance for these spectra is given by:

$$Z_{\text{tot}} = R_{\Omega} + \left(Q_1(\mathrm{j}\omega)^{n_1} + \frac{Q_2(j\omega)^{n_2}}{1 + R_1 Q_2(j\omega)^{n_2}} \right)^{-1} \tag{10}$$

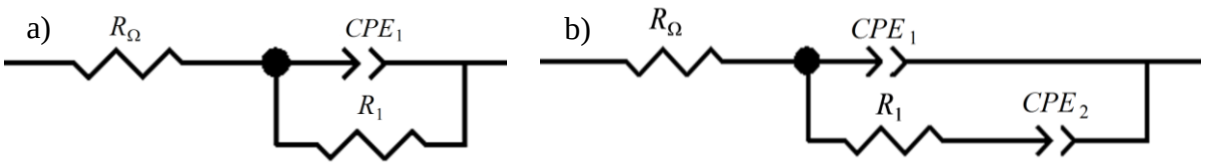

Figure 5. Electrical equivalent circuits used to fit the impedance spectra

Table 4. Impedance parameters for Fe electrode in a simulated acid rain solution, pH 4.5, in the absence and presence of AM extracts.

γ (AM extract)/ g L^{-1}	E_{OCP} / V	$Q_1 \cdot 10^{-6}$ / Ω^{-1} s^n cm^{-2}	n_1	R_1 / Ω cm^2	$Q_2 \cdot 10^{-6}$ / Ω^{-1} s^n cm^{-2}	n_2
-	–0.688	402.28	0.7163	972.57	-	-
0.01	–0.661	600.30	0.7237	1154.79	-	-
0.10	–0.650	468.70	0.7275	1371.34	-	-
0.50	–0.646	482.70	0.7662	4056.85	561.32	0.5435
1.00	–0.614	537.74	0.7064	4505.99	640.58	0.4906

As it can be seen from Table 4, the values of the open circuit potential in the presence of AM extracts were shifted in the positive direction relative to the OCP values in pure acid rain solution. From Table 4 it is evident that the impedance of the system increases from 1.15 to 4.50 kΩ cm^2 by increasing of AM extract concentration from 0.01 to 1.00 g $L^{-1.}$ High value of Q_1 and low value of n_1 point to the heterogeneity of the surface layer [42].

$$Z_{\text{tot}} = R_{\Omega} + \left(Q_1(j\omega) + \left(R_1 + \frac{R_2}{R_2 Q_2 (j\omega)^{n_2} + 1} \right)^{-1} \right)^{-1} \quad (11)$$

3.4. Atomic absorption spectrometry

The results obtained in the static immersion test are listed in Table 5. Generally, the dissolution of metal ions is dependent on the metal/alloy itself and the *pH* of the solution.

Table 5. The quantities of metal ions dissolved during 1 hour-immersion of bare metal specimens in simulated acid rain, pH 4.5, at E_{OCP} in the absence and presence of AM obtained by the AAS technique.

γ (AM extract)/ g L^{-1}	Quantity of released Fe (mg L^{-1} cm^{-2})
0	0.718
0.01	0.468
0.10	0.170
0.50	0.072
1.00	0.070

As can be seen from Table 5, a higher quantity of Fe was released from the iron immersed in the pure acid rain solution than from the iron immersed in the AM-containing solution. By increasing AM extract concentration, the quantities of released Fe ions are reduced. These results are in a good agreement with the results obtained by electrochemical techniques.

4. CONCLUSION

The influence of *Achillea millefolium* L. extract on the electrochemical behaviour of the iron in a simulated acid rain solution, pH 4.5, was investigated using electrochemical techniques, cyclic voltammetry, potentiodynamic polarization and electrochemical impedance spectroscopy.

Results of CV and PP showed that the *Achillea millefolium* L. extract adsorbed on the Fe and formed the thin layer at the Fe surface, which acts as a physical barrier preventing electrolyte action on the metal surface.

The inhibition efficiency increases with the increase of AM extract concentration. Adsorption of inhibitor molecules (from the AM extract) on the iron surface follows the Freundlich adsorption isotherm. The calculated free energy of adsorption (CV: $\Delta G° = -13.835$ kJ mol^{-1}; PP: $\Delta G° = -13.587$ kJ mol^{-1}) reveals a physical adsorption of the AM extract.

Results of impedance measurements at open circuit potential showed that AM extract contributes to iron passivation. The resistance values of the iron/oxide film/ (acid solution + AM extract) interface increase from 0.973 to 4.506 kΩ cm^2 by increasing AM concentration.

AAS results were in an accordance with results obtained by electrochemical techniques confirming that the increase in AM extract concentration (0.01 g L^{-1} – 1.00 g L^{-1}) decreases iron dissolution.

References

1. S.J. Ahn, H.S. Kwon and D.D. Macdonald, *J. Electrochem. Soc.,* 152 (2005) B482.
2. J. Dutta Majumdar and I. Manna, *Mater. Sci. Eng*., A 267(1) (1999) 50.
3. G. Meng, Y.Li, Y. Shao, T. Zhang, Y. Wang and F. Wang, *J. Mater. Sci. Technol*., 30 (2014) 253.
4. I. Martinović, Z.Pilić, I. Dragičević and A. Višekruna, *Int. J. Mater. Res*., 106 (2015) 1067.
5. I. Mišković and Z. Pilić, *Int. J. Electrochem. Sci*., 8 (2013) 7926.
6. S. Ningshen, U.K. Mudali and R.K. Dayal, *Br. Corros. J*., 36 (2001) 36.
7. S.F. Yang and D.D. Macdonald, *Electrochim. Acta*, 52 (2007) 1871.
8. L.J. Oblonsky and T.M. Devine, *Corros. Sci.*, 37 (1995) 17.
9. M. A. Amin, K.F. Khaled, Q. Mohsen and H.A. Arida, *Corros. Sci*., 52 (2010) 1684.
10. V. Schroeder and T.M. Devine, *J. Electrochem. Soc*. 146 (1999) 4061.
11. M.F. Toney, *Phys. Rev. Lett*., 79 (1997) 4282.
12. S. Marcelin, N. Pebere and S. Regnier, *Electrochim. Acta,* 87 (2013) 32.
13. L. Freire, X.R. Nóvoa, M.F. Montemor and M.J. Carmezim, *Mater. Chem. Phys*., 114 (2009) 962.
14. M.G.S. Ferreira, N.E. Hakiki, G. Goodlet, S. Faty, A.M.P. Simoes and M. Da Cunha Belo, *Electrochim. Acta,* 46 (2001) 3767.
15. S. Fujimoto and H. Tsuchiya, *Corros. Sci.,* 49 (2007) 195.
16. A. Kocijan, Č. Donik and M. Jenko, *Corros. Sci*., 49 (2007) 2083.
17. D.S. Azambuja, E.M.A. Martini and I.L. Müller, *J. Braz. Chem. Soc.,* 14 (2003) 570.
18. M. Bajt Leban, C. Mikyška, T. Kosec, B. Markoli and J. Kovač, *J. Mater. Eng. Perform*., 23 (2014) 1695.
19. F. Ahnia, Y. Khelfaoui, B. Zaid, F.J. Pérez, D. Miroud, A. Si Ahmed and G. Alcalá, *J. Alloys Compd*., 696 (2017) 1282.
20. Z. Pilić and I. Martinović, *Int. J. Mater. Res*., 107 (2016) 10.
21. M. Abdallah, A.Y. El-Etre, M.G. Soliman and E.M. Mabrouk, *Anti. Corros. Method* M., 53(2) (2006) 118.
22. Y.I. Kuznetsov, *Prot. Met*., 36 (2000) 128
23. A. Pardo, M.C. Merino, A.E. Coy, F. Viejo, R. Arrabal and E. Matykina, *Corros. Sci*., 50 (2008) 780.
24. A.S. Fouda and A.S. Ellithy, *Corros. Sci*., 51 (2009) 868.
25. A.Y. El-Etre, *J. Colloid Interface Sci*., 314 (2007) 578.
26. R. Babić, M. Metikoš-Huković, Z. Pilić, *Corrosion,* 59 (2003) 890.
27. S. Vitalini, G. Beretta, M. Iriti, S. Orsenigo, N. Basilico, S. Dall'Acqua, M. Iorizzi and G. Fico, *Acta Biochim. Pol*., 58 (2011) 203.
28. R.O. TeixeiraI, M.L. Camparoto, M.S. Mantovani and V.E.P. Vicentini, *Genet. Mol. Biol*., 26 (2003) 551.
29. G. Seufert, V. Hoyer, H. Wollmer and U. Arndt, *Environ. Pollut*., 68 (1990) 205.
30. L. Li, C. Wang, S. Chen, X. Yang, B. Yuan and H. Jia, *Electrochim. Acta,* 53 (2008) 3109.
31. M. Favre and D. Landolt, Proc. of the 7SEIC, Ann. Univ. Ferrara, N.S., Sez. V, *Suppl. N*., 9 (1990) 787.
32. R. Benetis, J. Radusiene, V. Jakstas, V. Janulis, G. Puodziuniene, A. Milasius, *Pharma. Chem. J.*, 42 (2008) 153.
33. M.Člupek, V. Prokopec, P. Matejka and K. Volka, J. Raman Spectrosc., 39 (2008) 515.
34. S. Sanchez-Cortes and J.V. Garcia-Ramos, *J. Colloid Interface Sci.,* 231 (2000) 98.
35. E. Sikora and D.D. Macdonald, *J. Electrochem. Soc*., 147 (2000) 4087.

36. S.K. Milonjić, *J. Serb. Chem. Soc*., 72 (2007) 1363.
37. A.B. Albadarin, C. Mangwandi, A.H. Al-Muhtaseb, G.M. Walker, S.J. Allen and M.N.M. Ahmad, *Chem. Eng. J.*, 179 (2012) 193.
38. J.R. Macdonald: Impedance spectroscopy, emphasizing solid materials and systems, Wiley, (1987), New York, USA.
39. E.M.A. Martini and I.L. Muller, *Corros. Sci*., 42 (2000) 443.
40. U. Rammelt and G. Reinhard, *Electrochim. Acta*, 35 (1990) 1045.
41. M. Metikoš-Huković, Z. Pilić, R. Babić and D. Omanović, *Acta Biomater*., 2 (2006) 693.
42. L. Vrsalović, S. Gudić and M. Kliškić, *Indian J. Chem. Technol*., 19 (2012) 96.